I&EC research
Industrial & Engineering Chemistry Research

Article

pubs.acs.org/IECR

Improving the Dynamic Properties of MRE under Cyclic Loading by Incorporating Silicon Carbide Nanoparticles

Yu Wang, Xinglong Gong,* Jie Yang, and Shouhu Xuan*

CAS Key Laboratory of Mechanical Behavior and Design of Materials, Department of Modern Mechanics, University of Science and Technology of China, Hefei 230027, People's Republic of China

ABSTRACT: A novel method was developed to enhance the cyclic performance of magnetorheological elastomers (MREs) by incorporating silicon carbide (SiC) nanoparticles. Different amounts of SiC nanoparticles were doped into the MREs, and their dynamic properties were investigated. In comparison to the neat MREs, the duration performance of SiC doped MRE was obviously improved. After the same cyclic loading, the maximum storage modulus and the magneto-induced storage modulus of the 4 wt % SiC-doped-MRE were approximately 1.1 and 1.3 times larger than the nondoped MREs. The maximum storage modulus, the magneto-induced storage modulus, and the MR effect in MRE-4 were approximately 1.73, 2.10, and 1.65 times that in MRE-0, respectively, after the cyclic load of different strain amplitudes. The improving mechanism was studied, and it was found that incorporating SiC nanoparticles can affect the stress distribution surrounding the magnetized carbonyl iron (CI) particles in the prestructure process and, thus, can affect the microstructures of the MREs.

1. INTRODUCTION

Fatigue behavior is different from monotonic loading; upon subjection to cyclic loading, a progressive and localized microscopic damage begins to form in materials.[1−3] Once the damage reaches a certain threshold, the structures will suddenly fracture. Therefore, the disastrous accidents caused by fatigue have drawn an increasing concern in many fields, especially in transportation. In particular, fatigue failure is a major discomfort that prevents the population of vibration devices made of polymer matrix composite materials, such as engine mount and seat mount. The polymer matrix around the filler particles was strained under loading, contributing to the increment of structural and thermal properties. However, upon application with a large or repeated load, the filler particles began to separate from the matrix and began to form microcracks. The microcracks coalesced with further loading and may ultimately result in noticeable cracks and in causing failure.[1,2]

Much research has been done to enhance the fatigue performance of polymer matrix composites. After systematically investigating the influence of deformation, testing environment, protective agent, and fillers on fatigue life and crack growth rate, Lake and Lindley[4] reported that the crack growth decreased by incorporating small carbon black. Legorju-jago and Bathias[5] investigated the influencing factors such as load ratio, temperature, thickness on the fatigue life, and crack rate, and they observed that the fatigue life of natural rubber (NR) increased in high load ratio or thickness. Hess and Ford[6] observed the formation of microcracks that originated from carbon black particles. Fröhlich et al.[7] analyzed the influence of carbon black and silica on the viscoelastic properties of rubber matrix composites, and they concluded that the modified in-rubber structure contributes to the enhancement in mechanical properties. Wolff et al.[8] reported that by filling carbon blacks, graphitized carbon blacks, silicas, and silica-modified organo-silanes into polymers, the filled polymer showed a higher compound viscosity and a higher modulus at low strain because of the polymer−filler and filler−filler interactions. Recently, SiC particles have become popular as the reinforcement phase for polymer.[9−12] Because of their well-dispersed property and good compatibility, the incorporation of SiC particles into polymer matrix can enhance the properties of polymer matrix composite.[11,12] Besides, SiC-reinforced materials retain their strength at high temperatures while providing better creep properties. It was reported that epoxy filled with 1.5% SiC nanoparticles showed an enhancement of mechanical properties about 20−30% in relation to pure matrix, both in tension and in flexure.[13]

As a kind of special polymer matrix composite, magneto-rheological elastomers (MREs) have drawn increasing attention in both industrial and academic areas because of their special magneto-induced properties. By applying a magnetic field, the ferromagnetic particles embedded in the matrix are magnetized and interact with the matrix, which makes the mechanical properties of MRE adjustable to external stimuli. Most of the present research on MREs was concentrated on the viscoelastic properties and their applications. Liu et al.[14] systematically investigated the different approaches for damping problems, and they pointed out that classic viscoelastic material showed the most desirable damping property. Lokander and Stenberg[15] reported that the relative MR effect increased with the addition of plasticizers, and the magnetic field also contributed to the increment of the relative MR effect before the iron particles magnetically saturated. By incorporating graphite to conventional MREs, Tian et al.[16] reported an increment in MREs' initial mechanical properties.

Considering that MRE-based devices are usually working in vibrational conditions, it is essential to comprehensively

Received: July 25, 2013
Revised: January 8, 2014
Accepted: February 5, 2014
Published: February 5, 2014

dx.doi.org/10.1021/ie402395e | *Ind. Eng. Chem. Res.* 2014, 53, 3065−3072

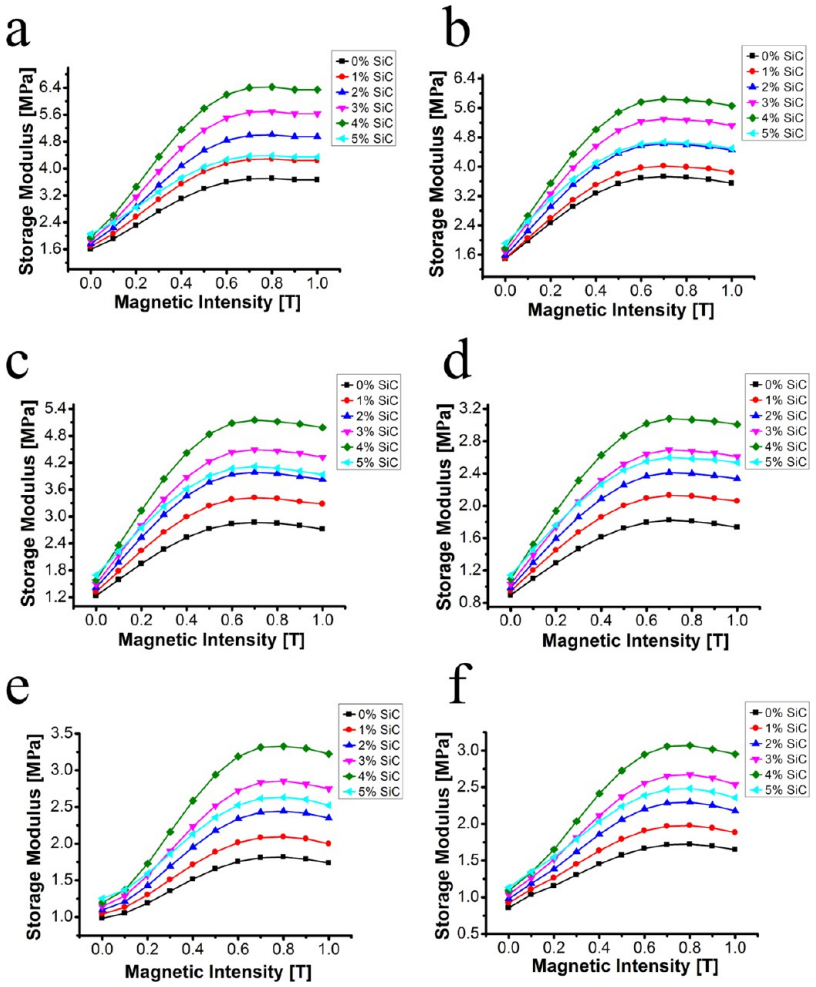

Figure 1. The storage modulus of different MRE samples after different load cycles, strain amplitude 50%: (a) without cycle load; (b) number of cycle 2×10^4; (c) number of cycle 4×10^4; (c) number of cycle 6×10^4; (d) number of cycle 8×10^4; (e) number of cycle 10×10^4.

investigate the durability of MRE after cyclic loads and to propose a solution to enhance its durability. Li et al.[17] utilized strain−stress loop area with magnetic field to evaluate the durability of MRE under different magnetic field intensities. Slawinski et al.[18] compared the mechanical performances of unprestructured and prestructured MRE after different cyclic loadings, and they concluded that the microstructure of the aligned particle chains can significantly affect the mechanical performance of MRE after the cyclic load. Zhang et al.[19] investigated the duration performance of a series of MRE samples based on mixed NR/*cis*-polybutadiene rubber (BR) when applied with the cyclic load, and they indicated that the durability of MRE containing more NR was better than the samples with more BR. They speculated that the network between the filler particles and the matrix was stronger in the NR-dominate MRE, and it was less likely to be broken after the cyclic load. Chen et al.[20] employed carbon black to generate a well-bonded microstructure, and it was reported that the mechanical properties of MRE were improved significantly.

In this paper, we focus on investigating the mechanical performance of SiC-filled MRE and MRE without SiC incorporated samples after being applied with the cyclic load. The results show that the mechanical performance of MREs incorporated with SiC nanoparticles is enhanced after cyclic load, and the enhanced performance of MRE doped with 4 wt % SiC nanoparticles is best under different cyclic load conditions. On the basis of the above results, the enhancing mechanism of the durability is discussed.

2. MATERIAL AND EXPERIMENTAL PROCEDURE

2.1. Sample Preparation. In this research, the natural rubber (NR) was used as the matrix, manufactured by the Hainan Rubber Group in China (type SCR WF). The magnetic particles were carbonyl iron (type CN) with an average diameter of 6 μm bought from BASF. A group of MRE samples were synthesized with different contents of 60 nm SiC nanoparticles, namely, 0, 1, 2, 3, 4, and 5 wt %. The carbonyl iron particles in each sample were equal (60 wt %), and the samples were named as MRE-0, MRE-1, MRE-2, MRE-3, MRE-4, and MRE-5, respectively. When the SiC nanoparticles were not mixed into MREs, the volume percentages of the particles were about 13.7%. The manufacturing procedures took three steps: first, the carbonyl iron (CI) particles, the SiC nanoparticles, and other additives were mixed via a double-roll mill, which ensured that all components were distributed homogeneously in the natural rubber matrix. Second, the products were compressed into a mold and were prestructured under an external magnetic field; after the prestructure, the CI particles formed patterned aligned aggregated structures in the matrix. Third, the products then were vulcanized to ensure that the aligned aggregated structures were locked into place in the matrix. SiC did not react with the NR rubber; however, as an

dx.doi.org/10.1021/ie402395e | Ind. Eng. Chem. Res. 2014, 53, 3065−3072

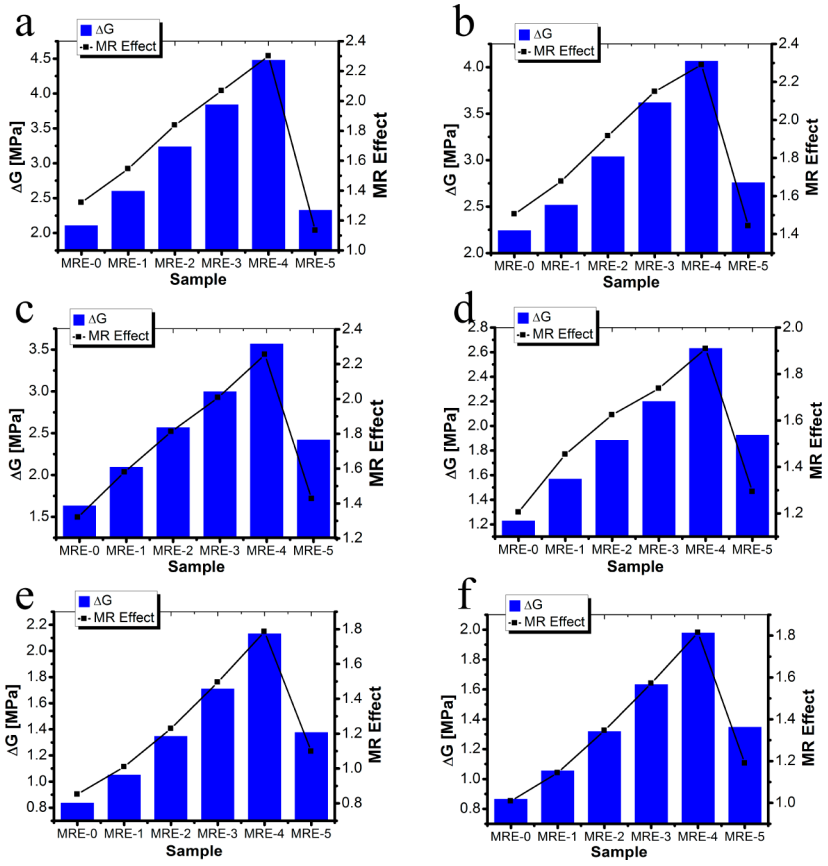

Figure 2. The magneto-induced storage modulus ΔG and MR effect of different MRE samples after different load cycles: (a) without cyclic load; (b) number of cycle 2×10^4; (c) number of cycle 4×10^4; (c) number of cycle 6×10^4; (d) number of cycle 8×10^4; (e) number of cycle 10×10^4.

ideal fortifier, it strengthened the matrix and improved the cyclic dynamic properties of the matrix. After all these procedures, the fabrications of the MRE samples were completed.

2.2. Cyclic Loading and Mechanical Characterization. The as-prepared products were cut into dumbbell shapes, 6 mm wide and 5.5 mm thick in the central area, following Chinese National Standard (GB 528-82). Then, the dumbbell-shaped samples were loaded with equibiaxial sinusoidal tension, and the frequency was 300 rad/min. The strain was displacement-controlled by a cyclic loading tester, JC-1008, Jiangdu Jingcheng Test Instruments Co. The cyclic load was conducted at room temperature, 23 °C. In the first group of tests, all samples were loaded with a sinusoidal tensile to evaluate the mechanical performances of these MRE samples under different load cycles. The load cycles were set as 0, 2×10^4, 4×10^4, 6×10^4, 8×10^4, and 10×10^4. The maximum displacement was 50% times its original length. In the second group of tests, all samples were applied with cyclic tensile stresses of different strain amplitudes. The maximum displacement was set as 25, 50, 75, and 100% times its original length, and the cyclic load was kept at 6×10^4. Then, the mechanical performance of each sample after cyclic load was measured with a modified dynamic mechanical analyzer (DMA). A self-made electromagnet was introduced to generate a variable magnetic field from 0 to 1000 mT, which was attached to a conventional DMA. In the experiments, the MRE samples had dimensions of 10 mm × 10 mm × 3 mm, and the particle chains were parallel with the thickness direction of sample. The direction of magnetic field was vertical to the load direction. The measuring tests were conducted at room temperature with a frequency of 10 Hz and a test strain of 0.2%. To eliminate the random errors, each group of tests was conducted five times under the same condition, and the average values were taken for analyzing. Both the load directions of DMA and the cyclic loading tester were all vertical to the iron particle chains. In this paper, each reported result is the averaged value of the three tests. Compared with the cyclic loading, whose frequency reached 300 rad/min, the relaxation was so slow that it was ignored. In addition, the morphology of these MRE samples were then characterized by utilizing scanning electron microscopy (SEM, Philips of Holland, model XL30 ESEM-TMP), operating at 20.0 kV.

3. EXPERIMENTAL RESULTS

3.1. Mechanical Performance of SiC-Filled MREs under Different Load Cycles. Because of their well-dispersed property and enhancement effect, the SiC nanoparticles were proven to be an ideal additive to strengthen the elastomeric materials. By introducing the SiC nanoparticles into the traditional MREs, the dynamic mechanical properties of the MRE materials were improved significantly. Figure 1 depicts the results of six different MRE samples after a series of load cycles. Regardless of the load cycles and the content of SiC nanoparticles, all samples showed significant MR behaviors, and the performances of samples incorporated with SiC were obviously enhanced compared to the sample without SiC doped. For example, in Figure 1a, the initial storage modulus G_0 increased from 1.62 MPa in sample MRE-0 to 2.08 MPa in sample MRE-5, which indicated the strengthening effect of SiC

dx.doi.org/10.1021/ie402395e | Ind. Eng. Chem. Res. 2014, 53, 3065−3072

nanoparticles. In addition, from Figure 1a to 1f, it can be observed that the mechanical performance of the samples with the same SiC nanoparticle content decreased as the load cycles increased, which follows the general depictions of material fatigue tests, and it was caused by the molecular network rapture in the matrix. However, after incorporating SiC nanoparticles, the decrement in mechanical performance that is due to fatigue was less obvious. The overall magneto-induced mechanical performances of the samples after cyclic load were better in the samples incorporated with SiC than in those without SiC nanoparticles. Notably, after experiencing the same number of cyclic loads, among all MRE samples incorporated with different contents of SiC nanoparticles or without SiC, the maximum storage modulus G_{max} peaked in the sample incorporated with 4% SiC. After the experiencing cyclic load for 0, 2×10^4, 4×10^4, 6×10^4, 8×10^4, and 10×10^4 rounds, the magneto-induced storage modulus ΔG of the sample MRE-4 was 1.13, 1.10, 1.15, 1.15, 1.17, and 1.16 times, respectively, that of the MRE-0. Furthermore, before the SiC incorporation rate arrived at 4%, the performance of the SiC-filled MRE increased with the SiC content. However, once the SiC weight fraction exceeded 4%, the magneto-induced mechanical performance sharply decreased. Form the six sets of tests (Figure 1a–f), regardless of the load cycles, the performance of MRE-5 was almost equal to that of MRE-3 or even decreased compared with that of MRE-3. For instance, in Figure 1a, the G_{max} of MRE-4 was 6.47 MPa, and the G_{max} of MRE-5 was 4.40 MPa, even smaller than 5.73 MPa of MRE-3.

The magneto-induced storage modulus and the absolute MR effect are key parameters to evaluate the performance of MREs. The MR effect is defined as $(G_{max} - G_0)/G_0$ in which G_0 is the initial modulus and the G_{max} is the maximal modulus during the test. Figure 2 and Figure 3 show the magneto-induced storage modulus ΔG and the MR effect of the six MRE samples incorporating different contents of SiC nanoparticles after experiencing different load cycles. As illustrated in Figure 2 and Figure 3, the magneto-induced performances also changed regularly with the content of SiC nanoparticles. It is obvious that all SiC-filled MRE showed an enhanced performance compared to the sample without SiC nanoparticles. After the same number of cyclic loads, both the magneto-induced storage modulus ΔG and the MR effect in the SiC-strengthened MRE are higher than that without SiC. This means that the SiC-strengthened MREs have a wider range of adjustable stiffness and can better respond to the stimuli with the existence of a magnetic field. In addition, the sample MRE-4 has the best enhanced effects.The ΔG and the MR effect increased with the weight content of SiC nanoparticles before the SiC incorporation rate reached 4%, and they decreased when the SiC content exceeded 4%. For instance, in Figure 2a , the ΔG of MRE-4 is 3.16 MPa, which is 2.10 times the value of MRE-0, which is 1.51 MPa, while the ΔG of MRE-5 is 1.62 MPa, which is only 1.07 times that of MRE-0. Similarly, the MR effect of MRE-4 is 212.4%, 1.69 times the 125.8% value in MRE-0. In addition, the MR effect of MRE-5 is 102.7%.

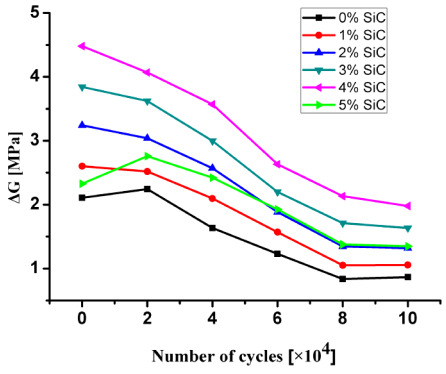

Figure 3. The change in storage modulus of MRE samples after different load cycles.

3.2. Performance of SiC Filled-MREs under Different Load Strain. In addition, to comprehensively understand the enhancement in the mechanical performance after cyclic loads, the MREs incorporating different weight contents of SiC nanoparticles were applied with cyclic loads of different strain amplitudes (25, 50, 75, 100% times their original length). The load circles were maintained to be 6×10^4. Then, the storage moduli of these samples were measured by utilizing DMA. The results are shown in Figure 4. Similarly, after cyclic load, all samples showed a typical MR behavior. In addition, the mechanical performances of the samples incorporating the same amount of SiC nanoparticles decreased with the strain amplitude. However, the decrement was less significant after incorporating SiC nanoparticles. The maximum storage modulus of MRE-4 was approximately 1.73 times that in MRE-0 after being loaded with cyclic strain with the same amplitude. More specifically, the initial storage modulus increased with the SiC nanoparticle content. The reinforcement effect was due to the large stiffness of the incorporated SiC nanoparticles. In addition, the maximum storage modulus of MRE-4 was larger than MRE samples incorporating any other content of SiC nanoparticles, that is, when the SiC weight fraction was lower than 4%, the maximum storage modulus G_{max} increased with the increasing of SiC content; when SiC content further increased, the G_{max} of SiC-filled MRE decreased, and the performance of MRE-5 was even lower than the sample of MRE-3. For instance, after cyclically loading under the strain amplitude of 100%, the G_{max} of MRE-4 was 2.85 MPa and the G_{max} of MRE-3 was 2.51 MPa, while the G_{max} of MRE-5 was 2.50 MPa. The magneto-induced storage modulus of MRE-4 was approximately 2.10 times that in MRE-0 under the same condition. This agrees well with the previous different load cycle tests. In addition, the magneto-induced performance and the MR effect also agreed well with the enhancement effect. On the one hand, with the increasing of the strain amplitude, the ΔG and the MR effect of the MRE samples incorporating the same amount of SiC nanoparticles decreased, for instance, when the strain amplitude was 25, 50, 75, and 100%, respectively, the corresponding ΔG of MRE-4 was 3.30, 2.66, 1.90, and 1.86 MPa and the MR effect was 213.9, 191.0, 180.6, and 188.7%. On the other hand, the maximum ΔG and the MR effect happened in sample MRE-4 (Figure 5). After application of cyclic strain with amplitude of 25%, the magneto-induced storage modulus increased from 1.50 MPa in MRE-0 to 3.30 MPa in MRE-4 and then decreased to 1.64 MPa in MRE-5. Similarly, the MR effect increased from 127.9% in MRE-0 to 213.7% in MRE-4 and then decreased to 103.6% in MRE-5.

4. DISSCUSSION

4.1. Morphology of Unmodified and Modified MRE. To comprehensively understand the incorporation of SiC nanoparticles on enhancing MREs' duration property, the morphology of the MRE samples and their microstructures

dx.doi.org/10.1021/ie402395e | Ind. Eng. Chem. Res. 2014, 53, 3065−3072

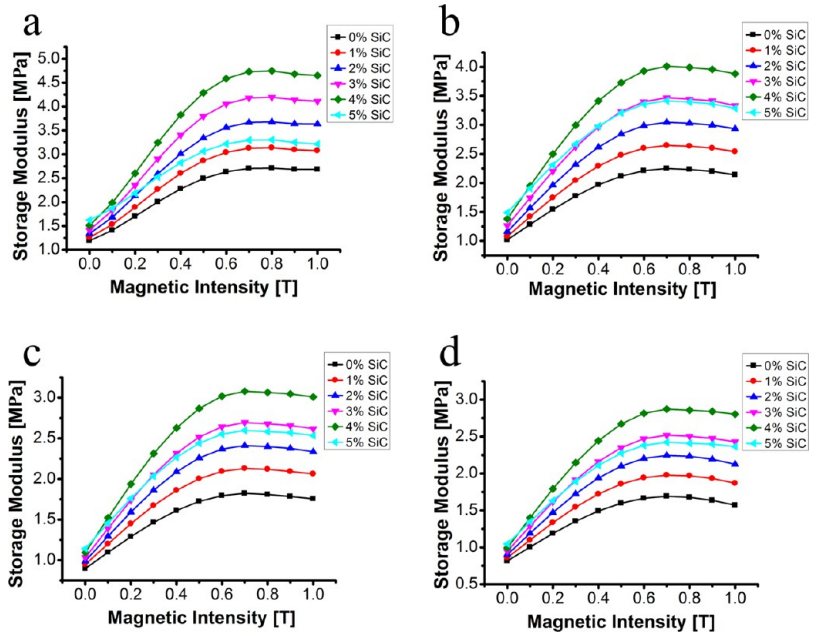

Figure 4. The storage modulus of different MRE samples after different cyclic strain amplitudes, load cycle 6×10^4. (a) Strain amplitude 25%, (b) strain amplitude 50%, (c) strain amplitude 75%, and (d) strain amplitude 100%.

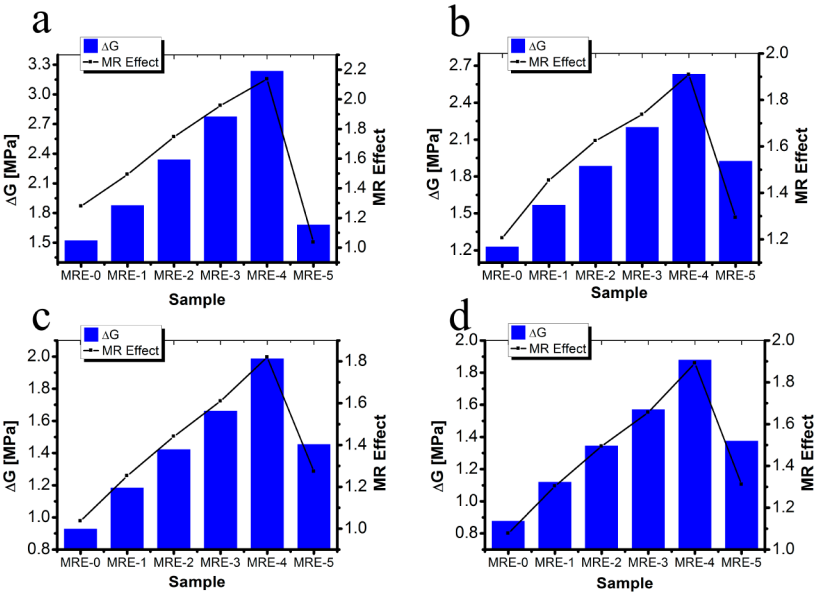

Figure 5. The magneto-induced storage modulus ΔG and the MR effect of different MRE samples under different cyclic strain amplitudes, load cycle 6×10^4. (a) Strain amplitude 25%, (b) strain amplitude 50%, (c) strain amplitude 75%, and (d) strain amplitude 100%.

were investigated via SEM, and the SEM images of the MRE samples are shown in Figure 6.

As illustrated in Figure 6, the iron particles are in white, and the NR rubber is in black. The average diameter of SiC particles was about 60 nm, which was much smaller than that of the CI particles, and so they cannot be seen in the SEM images. All the samples exhibited patterned chainlike structures, and the aligned structures bonded well with the rubber matrix. From Figure 6a to 5e, the configuration of the aligned chainlike structures became much more obvious and stouter. However, in MRE-5, the chainlike structures seemed to be disturbed, and the aligned structures were slimmer and less regular than that of the other samples. On the basis of the SEM observation, the microstructures of the aggregated structures in MRE were altered by the introduction of SiC nanoparticles into the manufacturing process. Before the SiC nanoparticle content exceeded the critical value, 4%, the SiC played a role in strengthening the aggregated structures. The aggregated structures in MRE appeared much stronger as the SiC content increased. However, once the weight content of SiC nanoparticles exceeded this critical value, the SiC nanoparticles interfered with the chain-formation process. Figure 6f shows that the aligned pattern was disturbed, and the aggregated structures were less obvious than that in MRE-4 and MRE-3. Therefore, the magneto-induced mechanical performance of MRE samples changed regularly with the SiC nanoparticle content. The SEM images of MREs after cycle loading were very similar to the images before, and microcracks did not

dx.doi.org/10.1021/ie402395e | Ind. Eng. Chem. Res. 2014, 53, 3065−3072

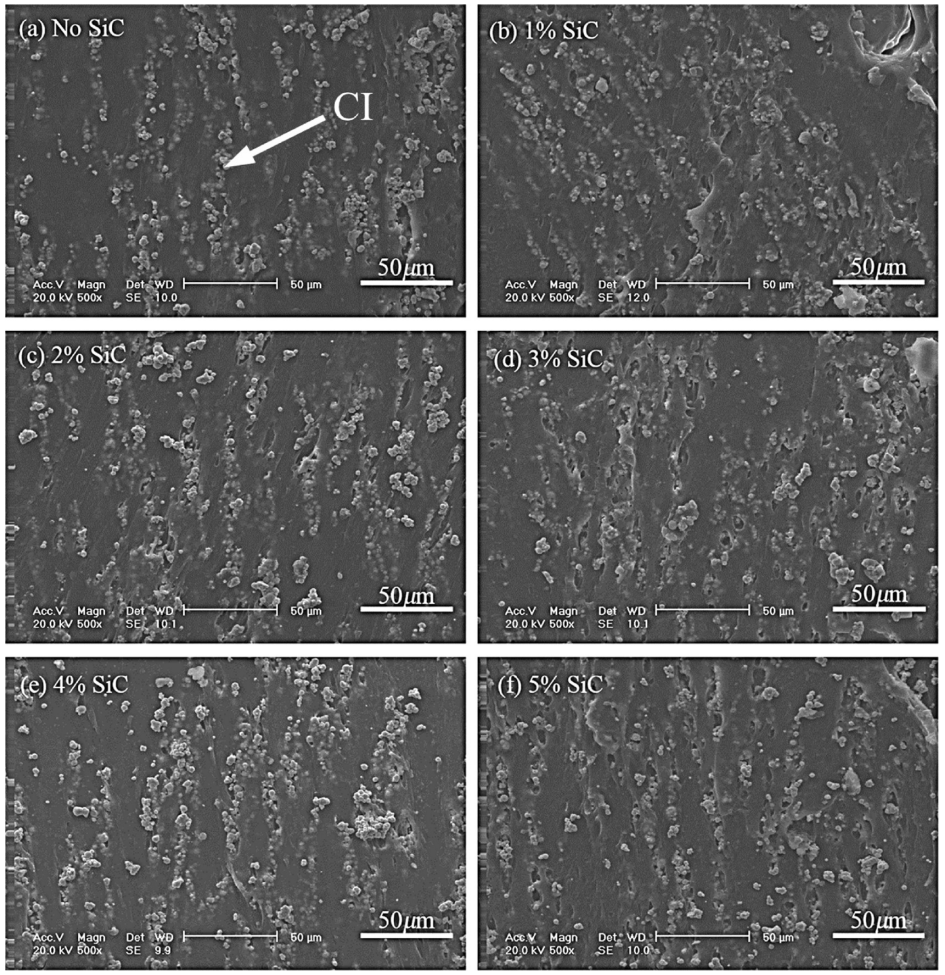

Figure 6. The SEM images of the six samples: (a) MRE-0, (b) MRE-1, (c) MRE-2, (d) MRE-3, (e) MRE-4, and (f) MRE-5.

appear in the matrix. It is speculated that the interface structure was changed, and cracks were very tiny; unfortunately, this cannot be observed by present experimental conditions.

4.2. Mechanism Study. On the basis of previous studies,[21,22] the storage modulus of MRE can be expressed as

$$G_{MRE} = G_0 + \frac{\varphi C d^3 A^2(\vec{H})(27\varepsilon^2 - 4\varepsilon^4 - 4)}{4r_0^3\mu_0\mu_1(1+\varepsilon^2)^{9/2}} \quad (1)$$

Here, G_0 is the initial storage modulus of MRE samples, ϕ is the content of carbonyl iron particles (CIPs), C is close to 1.2 in this study, d is the average diameter of the CIPs, $A(\vec{H})$ is the average magnetization intensity of CI particles when the external magnetic intensity is $\vec{H}$, ε is the scalar shear strain of the particle chain, r_0 is the average central distances between two adjacent CIPs, $\mu_0 = 4\pi \times 10^{-7}$ H·m^{-1} is the permeability of vacuum, and μ_1 is the relative permeability of the matrix material.

The average magnetization intensity $A(\vec{H})$ is the scalar dipole moment per particle volume, namely, $|\vec{m}| = A(\vec{H})\cdot V_i = (1/6)\pi d^3 A(\vec{H})$. The maximum magnetic-induced storage modulus occurs when the aligned particles become magnetically saturated, that is, $A(\vec{H}) = A(\vec{H})_{max}$. The saturation magnetization of carbonyl iron is known as $A(\vec{H})_{max} \approx 2.4$ T.[23] Therefore, the storage modulus of MRE is simplified as

$$(G_{MRE})^{max} = G_0 + \frac{1.728\varphi d^3(27\varepsilon^2 - 4\varepsilon^4 - 4)}{r_0^3\mu_0\mu_1(1+\varepsilon^2)^{9/2}} \quad (2)$$

In addition, the initial storage modulus is directely related to each component that constitutes the MRE sample. By utilizing the rule of mixture (ROM), the initial storage modulus can be expressed as

$$G_0 = (1 - \varphi - \phi)G_m + \varphi G_{p1} + \phi G_{p2} \quad (3)$$

Here, ϕ is the volume fraction of the CIPs, φ is the volume fraction of the SiC nanoparticles, G_m is the storage modulus of the matrix material, G_{p1} is the storage modulus of the CIPs, and G_{p2} is the storage modulus of the SiC nanoparticles.

Taking into account the concentrations,[24,25] the initial storage modulus of MRE samples should be corrected. However, the content of the SiC nanoparticles is too small to be considered. Therefore, the initial storage modulus of MRE samples is obtained as

$$G_0 = [(1 - \varphi - \phi)G_m + \varphi G_{p1} + \phi G_{p2}](1 + 2.5\varphi + 14.1\varphi^2) \quad (4)$$

Therefore, the storage modulus of the MRE before cyclic load is expressed as

dx.doi.org/10.1021/ie402395e | Ind. Eng. Chem. Res. 2014, 53, 3065−3072

$$G_{MRE} = [(1 - \varphi - \phi)G_m + \varphi G_{p1} + \phi G_{p2}] (1 + 2.5\varphi + 14.1\varphi^2) + \frac{\varphi C d^3 A^2(\vec{H})(27\varepsilon^2 - 4\varepsilon^4 - 4)}{4r_0^3\mu_0\mu_1(1 + \varepsilon^2)^{9/2}} \quad (5)$$

Cyclic load will decrease the storage modulus of the MRE samples, and the mechanical performance after cyclic load is given by[1−3,26,27]

$$\frac{G_{fatigue}}{G_{MRE}} = 1 - a\left(\frac{\sigma_{max}}{G_{MRE}}\right)^b\left(\frac{n}{N}\right)^c \quad (6)$$

here, a, b, and c are the experimental fitting constants, and σ_{max} is the maximum cyclic stress.

Generally, in this study, the duration performance of each sample after cyclic loads depended closely on the number of load cycles and on the strain amplitude. The mechanical performance of each sample decreased after different load cycles decreased with the number of the cyclic load and the cyclic strain amplitude. This agreed well with the prediction in eq 6. With the load cycles and strain amplitude increased, the network constituted by the reinforced particles and the matrix ruptured, causing the initial storage modulus to decrease with the load cycles.

In addition, on the basis of the experimental results and the aforementioned analyzed, the SiC nanoparticles worked as a strengthening agent for the mechanical performance of MRE samples. First, the initial storage modulus of each sample incorporated with SiC was higher than that without SiC. This can be explained by eq 4. As the weight content of the SiC nanoparticles increased, the initial storage modulus increased. This was due to the reinforced effect of the SiC nanoparticles. When loaded with strain, MRE deforms because of the deviation of the internal chainlike aggregate structures. However, the initial storage modulus of SiC nanoparticles is much larger than that of rubber matrix, and it is even larger than that of CIPs. Therefore, because of the SiC nanoparticles' extremely large stiffness, the deviation angles decreased with the increasing of SiC nanoparticles. As a result, the incorporation of SiC nanoparticles can significantly increase the initial storage modulus of the MRE samples.

Second, the mechanical performances of SiC-modified MRE, such as maximum storage modulus and magneto-induced storage modulus and MR effect, were better than that without SiC, which further demonstrated an ameliorated duration performance after cyclic load. In addition, the magneto-induced storage modulus and the MR effect behaved as a regular pattern: it increased until the SiC content reached the critical value 4%; after that, it sharply decreased as SiC nanoparticles further increased, and the performance of MRE-5 was even lower than that of MRE-3. However, the increased mechanical performance was actually the magneto-induced storage modulus. Considering the previous analysis, the regular changes of the mechanical performance were due to the changed microstructures of each MRE sample by incorporating SiC nanoparticles. In the process of prestructuring, the polymer matrix was in the molten state, and it was actually viscoplastic fluid, allowing the embedded particles to move around. Therefore, in the magnetic field, the embedded CI particles were magnetized in the prestructural magnetic field. By the drive of magnetic forces, the magnetized CI particles moved around and formed aligned aggregated structures, thus changing the flow field of the molten polymer matrix. Therefore, the movement of SiC nanoparticles was passive, and it was caused by the changed flow field. The movement of the magnetized CI particles changed the flow field of the molten polymer matrix and thus caused the SiC nanoparticles to move in the unstable flow field until reaching an equilibrium state. However, the velocity of the SiC nanoparticles was lower than that of the CI particles. As a result, the SiC nanoparticles attached to the surface of the CI particle chain and, in turn, formed a reinforced aggregated structure, which was indicated by the increasing of the initial storage modulus. Nevertheless, the passive movement of the SiC nanoparticles in the molten polymer flow field was slowed with the increasing of SiC nanoparticles. As the prestructure proceeded, the viscosity of the molten polymer increased gradually and fixed the CI particles into place, which means that the CI particles moved a comparatively shorter distance as the weight content of the SiC nanoparticles increased. Consequently, the aggregated structures composed of CI particles and SiC nanoparticles were much stronger as the SiC nanoparticles increased. However, when the SiC nanoparticles exceeded the critical value (in this experiment, it was 4%), the SiC nanoparticles, in turn, inhibited the movement of the CI particles, causing the CI particle chains to appear as a disturbed pattern.

5. CONCLUSION

In this paper, a group of MREs incorporated with different weight contents of SiC nanoparticles were fabricated, and their mechanical performances after cyclic loads were measured and analyzed. The results revealed that by incorporating SiC nanoparticles into fabricating MRE, the duration performance of MRE was enhanced. The initial storage moduli of the SiC-filled MRE were larger than the one without SiC nanoparticles. Notably, the maximum storage modulus, the MR effect, and the magneto-induced storage modulus changed regularly with the content of SiC nanoparticles: they increased before the SiC content reached 4 wt %, and they decreased sharply after the SiC nanoparticle content exceeded 4 wt %. After the same cyclic load cycles, the maximum storage modulus and the magneto-induced storage modulus in MRE-4 were approximately 1.13 and 1.30 times that in MRE-0, respectively. After the cyclic load of the same strain amplitude, the maximum storage modulus, the magneto-induced storage modulus, and the MR effect in MRE-4 were approximately 1.73, 2.10, and 1.65 times that in MRE-0, respectively. In addition, the mechanism of the enhanced duration performance was discussed. After incorporating SiC nanoparticles into MRE, stress distribution around the magnetic CI particles was altered in the prestructure process, thus changing the formation of aggregated structures and causing the magneto-induced performance of the as-prepared products to be changed.

AUTHOR INFORMATION

Corresponding Authors

*E-mail: gongxl@ustc.edu.cn. Tel: 86-551-3600419. Fax: 86-551-3600419.

*E-mail: xuansh@ustc.edu.cn. Tel: 86-551-3600419. Fax: 86-551-3600419.

Notes

The authors declare no competing financial interest.

■ ACKNOWLEDGMENTS

Financial support from the National Natural Science Foundation of China (Grant Nos. 11125210, 11072234, 11102202) and the National Basic Research Program of China (973 Program, Grant No. 2012CB937500) is gratefully acknowledged.

■ REFERENCES

(1) Kim, J.; Jeong, H. A study on the material properties and fatigue life of natural rubber with different carbon blacks. *Int. J. Fatigue* **2005**, *27*, 263−272.
(2) Woo, C. S.; Kim, W. D.; Kwon, J. D. A study on the material properties and fatigue life prediction of natural rubber component. *Mater. Sci. Eng., A* **2008**, *483*, 376−381.
(3) Tian, Z-h.; Tan, H.-f.; Du, X.-w. Fatigue properties of two kinds of rubber composites. *J. Mater. Eng.* **2008**, No. 6, 13−20.
(4) Lake, G. J.; Lindley, P. B. Ozone cracking, flex cracking and fatigue of rubber. *Rubber J.* **1964**, *146*, 24−30.
(5) Legorju-jago, K.; Bathias, C. Fatigue initiation and propagation in natural and synthetic rubbers. *Int. J. Fatigue* **2002**, *24*, 85−92.
(6) Hess, F. M.; Ford, F. P. Microcopy of pigment−elastomer systems. *Rubber Chem. Technol.* **1963**, *36*, 1175−1229.
(7) Frohlich, J.; Niedermeier, W.; Luginsland, H. D. The effect of filler-filler and filler-elastomer interaction on rubber reinforcement. *Composites, Part A* **2005**, *36*, 449−460.
(8) Wolff, S.; Tan, E. H.; Donnet, J. B. The effect of filler surface-energy on dynamic properties. *Kaut. Gummi Kunstst.* **1994**, *47*, 485−492.
(9) Colomban, P. Analysis of strain and stress in ceramic, polymer and metal matrix composites, by Raman spectroscopy. *Adv. Eng. Mater.* **2002**, *4*, 535−542.
(10) Interrante, L. V.; Moraes, K.; Sherwood, W.; Jacobs, J.; Whitmarsh, C. In *Low cost, near net shape ceramic composites by polymer infiltration and pyrolysis*, Proceedings of the Eighth Japan-U.S. Conference on Composite Materials, Baltimore, MD, 1998; Newaz, G. G., Gibson, R. F., Eds.; Technomic Publishing Company, Inc.: Lancaster, PA, 1998; pp 506−515.
(11) Shao, S. Y.; Yang, P.; Wang, G.; Zhang, J. The preparation and attributes of SiC&Natural rubber. *Chem. Ind. Times (Chinese)* **2010**, *24*, 25−36.
(12) Kueseng, K.; Jacob, K. I. Natural rubber nanocomposites with SiC nanoparticles and carbon nanotubes. *Eur. Polym. J.* **2006**, *42*, 220−227.
(13) Rodgers, R. M.; Mahfuz, H.; Rangari, V. K.; Chisholm, N.; Jeelani, S. Infusion of SiC nanoparticles into SC-15 epoxy: An investigation of thermal and mechanical response. *Macromol. Mater. Eng.* **2005**, *290*, 423−429.
(14) Liu, Y.; Sánchez Cebrián, A.; Zogg, M.; Ermanni, P. A comparative experimental study on structural and interface damping approaches for vibration suppression purposes. *Proc. SPIE* **2010**, *7643*, 764335/1−764335/10.
(15) Lokander, M.; Stenberg, B. Improving the magnetorheological effect in isotropic magnetorheological rubber materials. *Polym. Test.* **2003**, *22*, 677−680.
(16) Tian, T. F.; Li, W. H.; Alici, G.; Du, H.; Deng, Y. M. Microstructure and magnetorheology of graphite-based MR elastomers. *Rheol. Acta* **2011**, *50*, 825−836.
(17) Li, W. H.; Zhang, X. Z.; Du, H. P. Development and simulation evaluation of a magnetorheological elastomer isolator for seat vibration control. *J. Intell. Mater. Syst. Struct.* **2012**, *23*, 1041−1048.
(18) Slawinski, G.; Miedzińska, D.; Niezgoda, T.; Boczkowska, A. Experimental investigations of MREs behavior under the cyclic load. *Solid State Phenom.* **2011**, *183*, 163−168.
(19) Zhang, W.; Gong, X. L.; Jiang, W. Q.; Fan, Y. C. Investigation of the durability of anisotropic magnetorheological elastomers based on mixed rubber. *Smart Mater. Struct.* **2010**, *19*, 085008/1−085008/11.
(20) Chen, L.; Gong, X. L.; Li, W. H. Effect of carbon black on the mechanical performances of magnetorheological elastomers. *Polym. Test.* **2008**, *27*, 340−345.
(21) Zhu, Y. S.; Gong, X. L.; Dang, H.; Zhang, X. Z.; Zhang, P. Q. Numerical analysis on magnetic-induced shear modulus of magneto-rheological elastomers based on multi-chain model. *Chin. J. Chem. Phys.* **2006**, *19*, 126−130.
(22) Shen, Y.; Golnaraghi, M. F.; Heppler, G. R. Experimental research and modeling of magnetorheological elastomers. *J. Intell. Mater. Syst. Struct.* **2004**, *15*, 27−35.
(23) Jolly, M. R.; Carlson, J. D.; Munoz, B. C. A model of the behaviour of magnetorheological materials. *Smart Mater. Struct.* **1996**, *5*, 607−614.
(24) Guth, E. Theory of filler reinforcement. *Rubber Chem. Technol.* **1945**, *18*, 596−604.
(25) Davis, L. C. Model of magnetorheological elastomers. *J. Appl. Phys.* **1999**, *85*, 3348−3351.
(26) Zhang, W.; Gong, X. L.; Sun, T. L.; Fan, Y. C.; Jiang, W. Q. Effect of cyclic deformation on magnetorheological elastomers. *Chin. J. Chem. Phys.* **2010**, *23*, 226−230.
(27) Qi, H. Y.; Wei, W. D.; Sun, L. W. Fatigue damage accumulation model based on stiffness degradation. *J. Beijing Univ. Aeronaut. Astronaut.* **2004**, *30*, 1200−1203.